

CMOS-MEMS capacitive tactile sensor with vertically integrated sensing electrode array for sensitivity enhancement

Meng-Lin Hsieh^a, Sheng-Kai Yeh^a, Jia-Horng Lee^a, Ming-Ching Cheng^a, Weileun Fang^{a,b,*}

^a Power Mechanical Engineering, National Tsing Hua Univ., Hsinchu, Taiwan

^b Institute of NanoEngineering and MicroSystems, National Tsing Hua Univ., Hsinchu, Taiwan

ARTICLE INFO

Article history:

Received 12 May 2020

Received in revised form 28 August 2020

Accepted 10 September 2020

Available online 24 November 2020

Keywords:

Tactile sensor

Sensitivity enhancement

Capacitive

Vertical integration

ABSTRACT

This study presents the design, fabrication, and testing of a novel capacitive type CMOS-MEMS tactile sensor with vertically integrated sensing structures for enhancing sensitivity, and discretized sensing array design for inhibiting residual stress warpage. The proposed type tactile sensor utilizes polymer buffer above the sensor and polymer fill-in between the vertically integrated sensing structures as force transmission layers. This enables effective force loading onto the sensor, and more importantly, simultaneous deformation of the two vertically integrated sensing structures during force loading, thereby guaranteeing an increase in sensitivity. The enhancement in sensitivity of the proposed tactile sensor was demonstrated to be achieved under the same footprint area. To mitigate warpage issues that may occur due to thin film residual stresses, the sensor was discretized into arrays of separate sensing units. Sensing units are electrically connected in a parallel fashion to ensure maximum capacitance signal. As compared to a reference tactile sensor with conventional sensing electrodes, the proposed design showed a near 1.3-fold enhancement in sensitivity. Measurements also indicate the 5×5 array design could tolerate the influence of residual stress. Additionally, effect of operating temperature on initial capacitance (temperature coefficient of offset, TCO) and capacitance change signal during force loadings (temperature coefficient of sensitivity, TCS) were investigated for both the reference and proposed type tactile sensors.

© 2020 Elsevier B.V. All rights reserved.

1. Introduction

Tactile sensors are widely utilized in various fields, such as in consumer electronics, robotics industry, or in medical applications. For example, tactile sensors have been utilized as control interfaces for consumer electronics as in functions keys in earbuds [1]; tactile sensors can also be incorporated onto robotics to enable tactile sensing capabilities which, by providing additional sensing information, achieve enhancement in performance through force sensing or even slippage, hardness, topography, and imaging [3,4]. Moreover, tactile sensors can be integrated onto medical tools for minimal invasive surgeries such as laparoscopy to provide, on top of traditional imaging techniques, tactile information that may benefit surgery quality and safety [5]. In these applications, the pursuit of further miniaturization and cost reduction has paved way for micro-electro-mechanical-systems (MEMS) tactile sensors, which,

due to the batch micromachining fabrication techniques, possess these much-required benefits.

Capacitive sensing is regarded as a promising approach for MEMS tactile sensors [6–13]. Various sensing mechanisms such as gap-closing [6–12], area-changing [9], or fringing effect [13] have been employed for capacitive tactile sensors. Since the gap-closing sensing mechanism has the advantages of high sensitivity and relatively ease of fabrication, it has been extensively applied in capacitive tactile sensors. Many approaches have been reported to further enhance the sensitivity of the gap-closing tactile sensors [8,7–12]. For example, material fill-ins with different mechanical properties were investigated to improve the sensitivity of gap-closing tactile sensor [8,9]. By varying the dielectric constant and stiffness of gap-closing tactile sensor using fill-ins, the sensitivity can be modulated. Moreover, many different structural designs, such as nano-needles, pyramids, or escape outlets, were also presented to improve the sensitivity of gap-closing tactile sensor [10,7–12]. When compared to completely filled in gaps, these structural designs can enable the released electrode to more easily deform, hence achieving higher sensitivities. To vertically integrate multiple sensing electrodes (in parallel) is a simple approach to

* Corresponding author at: Power Mechanical Engineering, National Tsing Hua Univ., Hsinchu, Taiwan.

E-mail address: fang@pme.nthu.edu.tw (W. Fang).

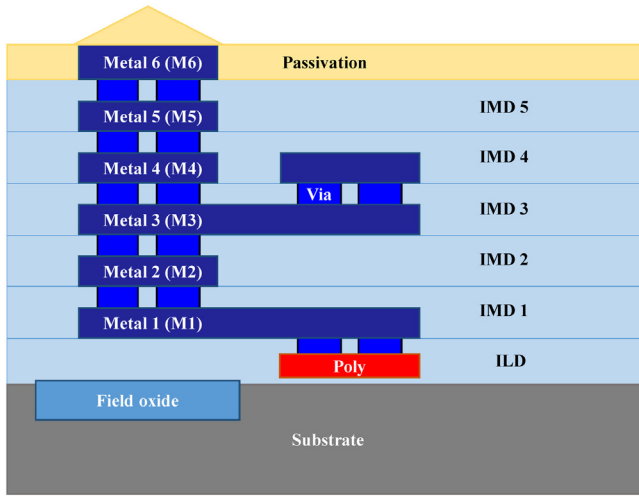


Fig. 1. Layer stacking for the TSMC 0.18 μm 1P6M CMOS process.

increase the sensing capacitance of the gap-closing tactile sensors. However, the stacking of thin film layers is required for realizing multiple sensing electrodes and the complicated electrical routing needed poses fabrication issues. In addition, the force transmission between different sensing layers is still another design concern.

The complementary metal-oxide-semiconductor (CMOS) processes have been developed for more than a few decades, and are mature fabrication technologies to date. Many standard CMOS processes are available in commercial foundries, for example, the TSMC (Taiwan Semiconductor Manufacturing Co.) 0.18 μm 1P6M (one poly and six metal layers) CMOS process shown in Fig. 1. Such a standard CMOS process offers many dielectric and metal layers on top of the Si substrate, and provides connecting vias to electrically connect between layers. The monolithic integration of suspended MEMS structures for various applications have been demonstrated in [2,7,8,14–16]. Thus, the CMOS process is a promising approach to vertically integrate multiple sensing electrodes (in parallel) to enhance the sensing capacitance of the gap-closing tactile sensor. Extended from the approach in [17], this study leverages the fabrication advantages of the CMOS process to realize a gap-closing capacitive tactile sensor with multiple vertically integrated sensing electrodes in an array to achieve enhancements in sensitivity performance. The proposed sensor includes three layers of vertically integrated sensing electrodes, and these sensing electrodes were then configured in a parallel fashion utilizing the electrical routing capabilities of the CMOS process. In addition, the molding process is employed to fabricate polymer buffer and polymer fill-in layers for transmitting force between layers. Moreover, this study also presents the array type tactile sensing elements design for inhibiting residual stress warpage of the suspended MEMS structures.

2. Design concepts and principles

Based on the available layers for the TSMC standard 0.18 μm 1P6M CMOS process shown in Fig. 1, this study presents the tactile sensor design illustrated in Fig. 2. As displayed in Fig. 2a, the proposed tactile sensor consists of a CMOS sensing chip, a polymer buffer, and a glass bump. The tactile force to be detected will be applied on the rigid glass bump which serves as the force contact interface (tactile bump). An intermediate flexible polymer buffer is used to help transmit the load from the rigid glass bump to the deformable thin film structures of each sensing element on the CMOS chip, thus leading to changes of the sensing gaps. Also, this polymer buffer acts as a protection layer to the fragile thin film structures on the CMOS chip. As shown in Fig. 2b, the tactile sensor

is comprised of three vertically integrated structures with polymer filled in between, and configured in an array form with discretized sensing units. The vertically integrated structure is consisted of the dielectric and metal layers. The metal layers (M1, M3, and M5 in Fig. 1) embedded in the dielectric films serve as the sensing electrodes. The top and middle structures are deformable square plates with four edges clamped (except at the etching release holes). The bottom structure, which serves as the fixed electrode, is fully anchored to the substrate. The polymer fill-in between vertically integrated structures is exploited to transmit the tactile load between these layers. In comparison, the conventional capacitive type tactile sensors typically adopt a double-sensing-electrode design with only a single deformable layer. Under tactile loadings, with the polymer fill-in present for force transmitting, the top and middle structures will be deformed simultaneously, thereby changing the two gap distances between the three sensing electrodes. Force sensing is then carried out by the gap-closing induced capacitive signal. Note the initial gaps between sensing electrodes are determined by the thicknesses of sacrificial metal layers (M2 and M4 in Fig. 1). Thus, the thicknesses of sensing gaps are constrained by the design rules of TSMC. This study discretizes the single sensing element into array type sensing units while having the same chip size. The array type design could reduce the size of suspended structures for each sensing elements, and further reduce their initial deflection amplitudes resulted from the thin film residual stresses [19,20]. Thus, the contact or stiction of sensing electrodes and the significant change of sensing gap due to the warpage of the suspended structures can be prevented. The sensing signal of each unit can be combined through electrical routings. As depicted in both the top and cross section views, the metal connections (in light blue color) serve to electrically route the capacitance signals of discrete sensing units for summation. A chip with 5×5 tactile sensing array is used as an example in Fig. 2 to show the architecture of the presented design. Moreover, the holes for etching release of sacrificial metals that are filled with polymer are also depicted in the figure.

Fig. 3a further illustrates the working principle of the proposed vertically integrated three sensing electrodes. For comparison, the conventional design with two sensing electrodes is also displayed. An individual sensing unit within the array is employed as an example, and the cross section schematics are shown. The two gaps in between the electrodes are initially at heights of h_0 and the two pairs of capacitors have initial capacitances of C_0 . When external force is applied, the polymer buffer and fill-in act as force transmission layers which allow for simultaneous deformation of the released structures, resulting in a reduction in initial gap heights between the electrodes. Therefore, the initial gap heights h_0 at the center of the sensing electrodes are respectively reduced to h_1 and h_2 and capacitance changes of ΔC_1 and ΔC_2 are induced from the two pairs of capacitors. As shown in the electrical model in Fig. 3b, the induced capacitance changes can then be summed through a parallel configuration of the sensing electrodes, and hence the net capacitance change of each sensing unit ΔC_{unit} is expressed as,

$$\Delta C_{unit} = \Delta C_1 + \Delta C_2 \quad (1)$$

Note that in this proposed design, the top electrode will have a larger deformation than that of the middle electrode, guaranteeing an increase in capacitance change for both sensing pairs during external loads, or in other words $h_1 < h_0$ and $h_2 < h_0$. Thus, both sensing pairs can contribute positively to the enhancement of the capacitive signal. As compared to the reference type (double sensing electrodes) with central gap height reduced from h_0 to h_3 by the tactile load, the proposed design induces a larger capacitance change ($\Delta C_1 + \Delta C_2 > \Delta C_3$), and thus a sensitivity enhancement. Moreover, no additional sensor footprint is required due to the vertical integration of sensing electrodes. The capacitance changes of individual sensing units within the array, ΔC_{unit} , can be further

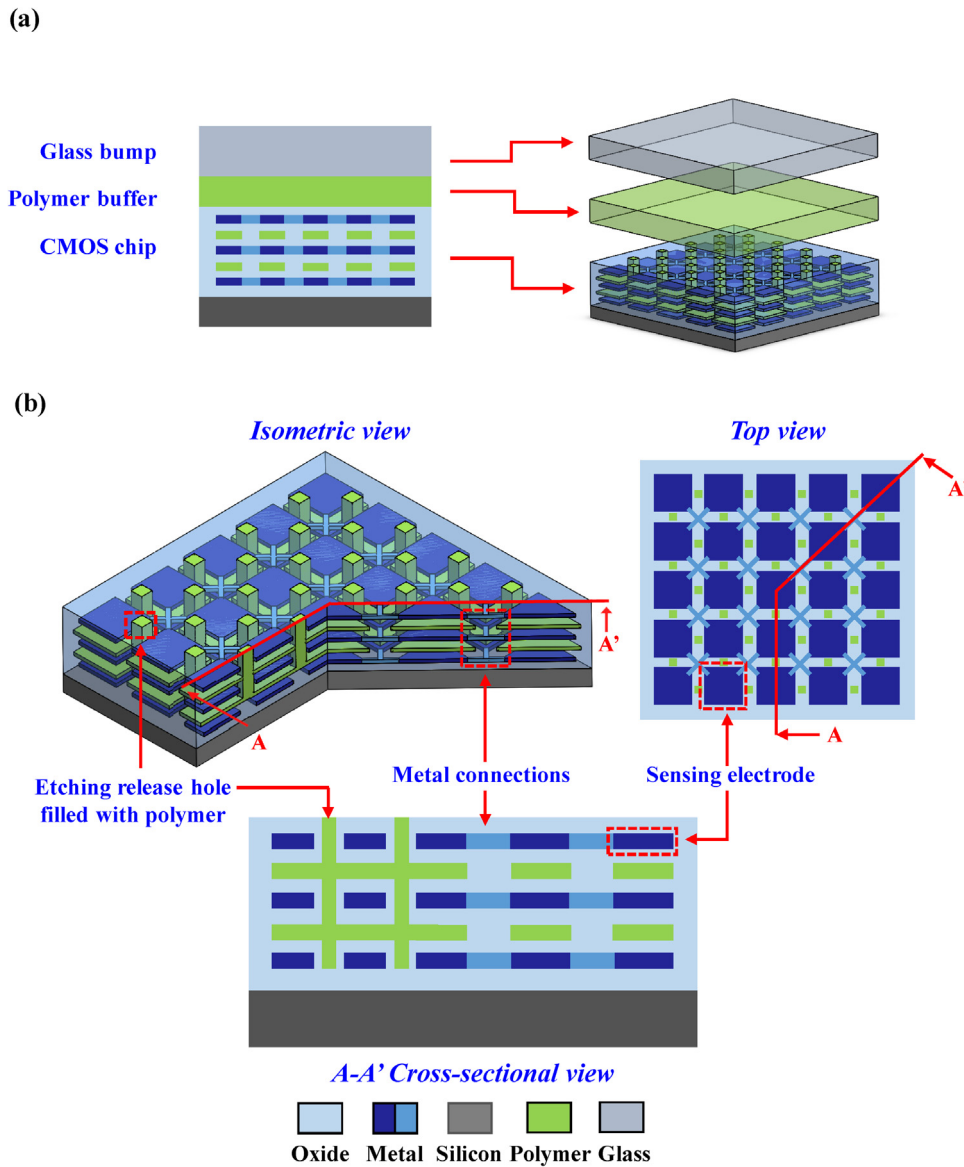


Fig. 2. (a) Cross section and exploded view of the sensor components, (b) schematic of the proposed tactile sensor in isometric view, top view, and cross-sectional view.

summed with a parallel configuration to obtain the total capacitance change, $\Delta C_{effective}$, of the proposed tactile sensor as,

$$\Delta C_{effective} = n \times \Delta C_{unit} \quad (2)$$

Where n is the total sensing elements in the array. Considering the complicated electrical routing and layer stacking required due to the vertical integration and discretized array, the multiple benefits of the standard CMOS platform was leveraged to fabricate the tactile sensors in this study. By using the 5×5 array type tactile sensor shown in Fig. 2 as an example, each sensing unit will require three vertically stacked metal electrodes. Thus, the tactile sensor array has totally 75 sensing metal electrodes. These 75 sensing metal electrodes must be electrically connected to form a parallel configuration to ensure the maximum capacitance readout. Therefore, the CMOS platform with its exceptional routing capabilities and multi-stacked metal and dielectric layers provides a simple solution to realize the proposed designs.

Finite element method (FEM) analysis by using the commercial FEM software (COMSOL Multiphysics®) was conducted as a preliminary evaluation of the effects of the proposed design, and the results are shown in Fig. 4. As shown in Fig. 4a, the simulation

model (with in-plane dimensions of $1000 \times 1000 \mu\text{m}^2$) includes the glass bump, the polymer buffer, and the sensing die (containing 5×5 sensing units with total footprint of $630 \times 630 \mu\text{m}^2$). In addition, the FEM model of each sensing unit consists the metal and dielectric layers, the silicon substrate, and the polymer fill-in, and a Mooney-Rivlin hyperelastic material model ($C_{10} = 0.0625 \text{ MPa}$, $C_{01} = 0.1 \text{ MPa}$) was incorporated to represent the polymer employed [21]. After applying uniform distributed load on the glass bump, the deflection profiles of suspended structures with embedded sensing electrodes are predicted by the FEM simulation. Simulation results in Fig. 4b depict the typical central gap heights h_1 , h_2 , and h_3 (also indicated in Fig. 3a) of deformable structures varying with different uniform distributed loads. Such typical results are determined from the center sensing unit of the 5×5 array. Note the variation of deformation between sensing units of the array is tiny (approximately two orders of magnitude smaller). As the force increases, reductions in central gap heights, from an initial value h_0 of $0.53 \mu\text{m}$, can be observed across all three gaps of both tactile sensors as the released structures gradually deform. Due to the nonlinear behavior of the hyperelastic model incorporated for the polymer fill-in, the change in gap height saturates for

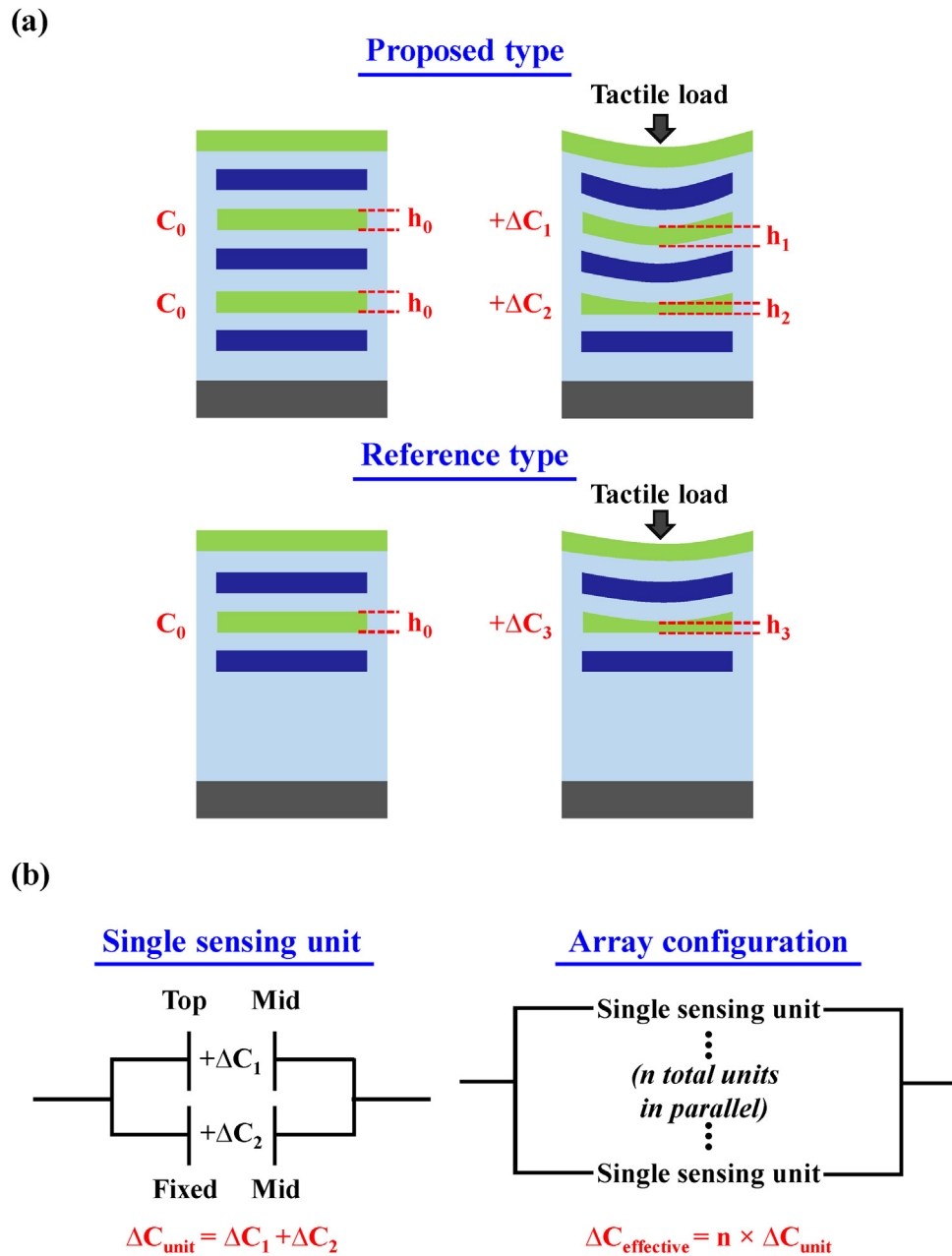


Fig. 3. (a) The single sensing unit deforming schematics of the working principle for the proposed and reference type tactile sensors, and (b) the electrical model for a single sensing unit and array configured proposed type tactile sensor.

all three gaps. Simulation results in Fig. 4c further present the total capacitance changes (from 25 sensing units) of the proposed and reference tactile sensors at different loads. The results show a gradual increase in capacitance signal as the membrane is deformed and gaps between sensing electrodes are decreased. As the gap change gradually saturates as shown in Fig. 4b, the capacitance signal also saturates. Note that the cause of this signal nonlinearity differs from gap-changing capacitive sensors with air in between the sensing electrodes. The results show a less than 1% nonlinearity for the proposed design within the loading range (15 N) of the humanoid robotics applications [18]. More importantly, in comparison with the reference design, the proposed one increased the sensitivity (capacitance change/force) by around 1.5-fold. In conclusion, under the loading range of 15 N, the proposed design can increase sensitivity performance while maintaining a linear capacitance response.

3. Fabrication and results

Fig. 5 shows the fabrication process of the proposed sensor. Fig. 5a displays the chip fabricated by the TSMC 0.18 μm 1P6M standard CMOS process. The metal and dielectric oxide layers, connecting vias, and silicon substrate are depicted in the figure. After the chip preparation by the foundry, post fabrication steps which include metal wet etching, laser pad opening, wire bonding, and polymer molding processes followed. This study designed two types of test keys. The first type is to monitor the respective wet etching of the two sacrificial metal layers (M2, and M4), and the other is to monitor the presence of the sensing electrodes layers (M3 and M5). Since the metal layer is covered by the transparent silicon dioxide layers, the etching status as well as the sensing electrodes can be observed by the microscope. Fig. 5b illustrates the metal wet etching process. In this step, the vertically

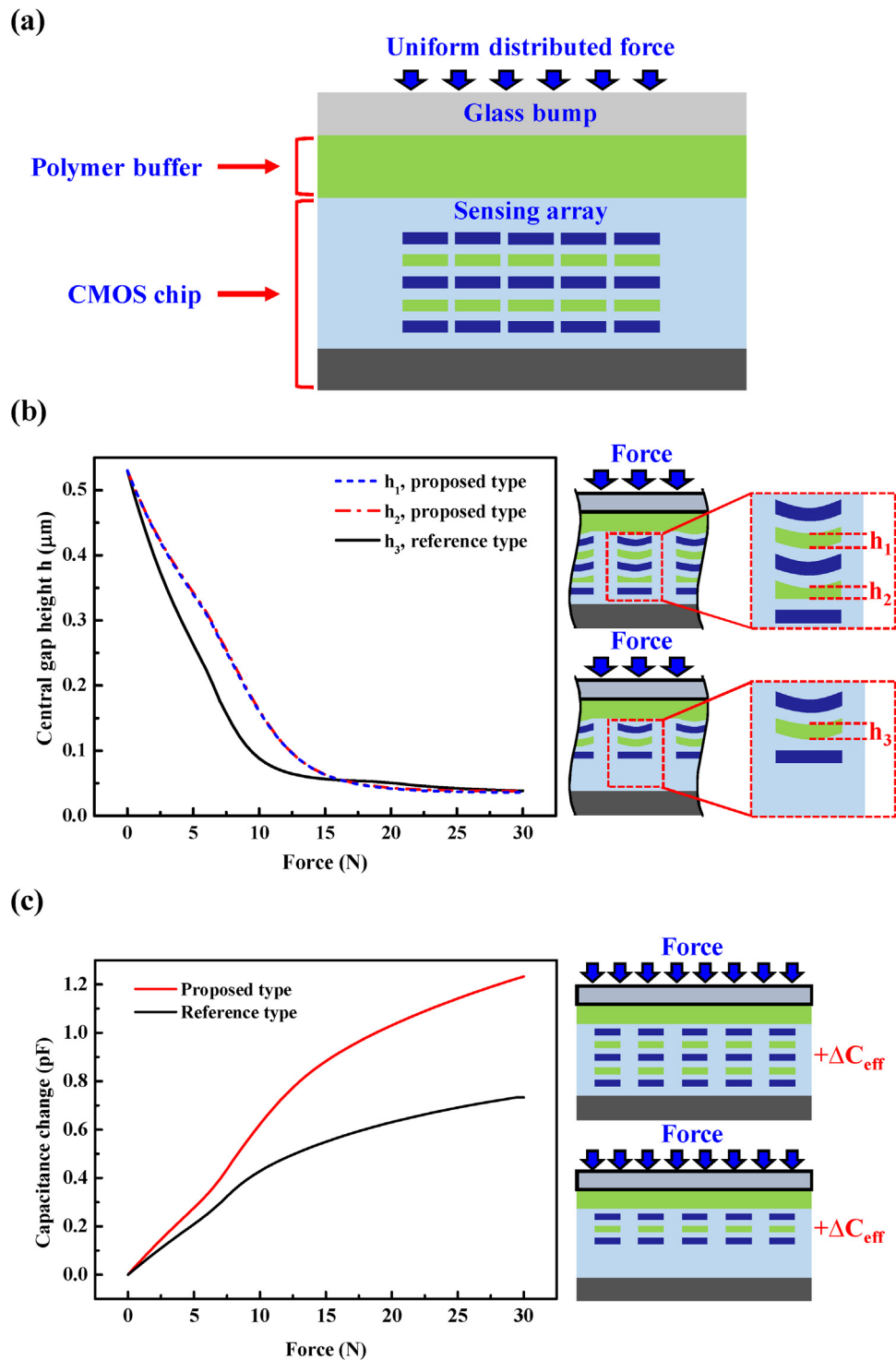


Fig. 4. (a) Simulation model and the simulation results of (b) the central gap height, and (c) the overall capacitance change under force loadings for the proposed and reference types.

integrated structures and individual sensing units of the tactile sensor were defined and released, and the embedded metal sensing electrodes were protected with silicon dioxide dielectric layers [22]. Following the metal wet etching, laser machining was utilized to remove the silicon dioxide layer to expose pads for wire bonding. As shown in Fig. 5c, the wire bonding and epoxy protection processes were then performed on the printed circuit board (PCB). The polymer molding process was used to encapsulate the sensing chip, as illustrated in Fig. 5d. In this study, polydimethyl-

siloxane (Dow Corning® SYLGARD PDMS 184, curing ratio 10:1) is employed. The metal mold was placed on the PCB to define the height and shape of the molded PDMS. Before curing, the PDMS was placed in a vacuum chamber to ensure the air bubbles are not trapped within the sensing structures. Then, the PDMS is cured at 120°C for 30 min. The typical fabricated tactile sensor has a polymer buffer thickness of $200 \pm 10 \mu\text{m}$. After curing, the bulk glass was assembled to serve as the tactile bump for the presented sensor.

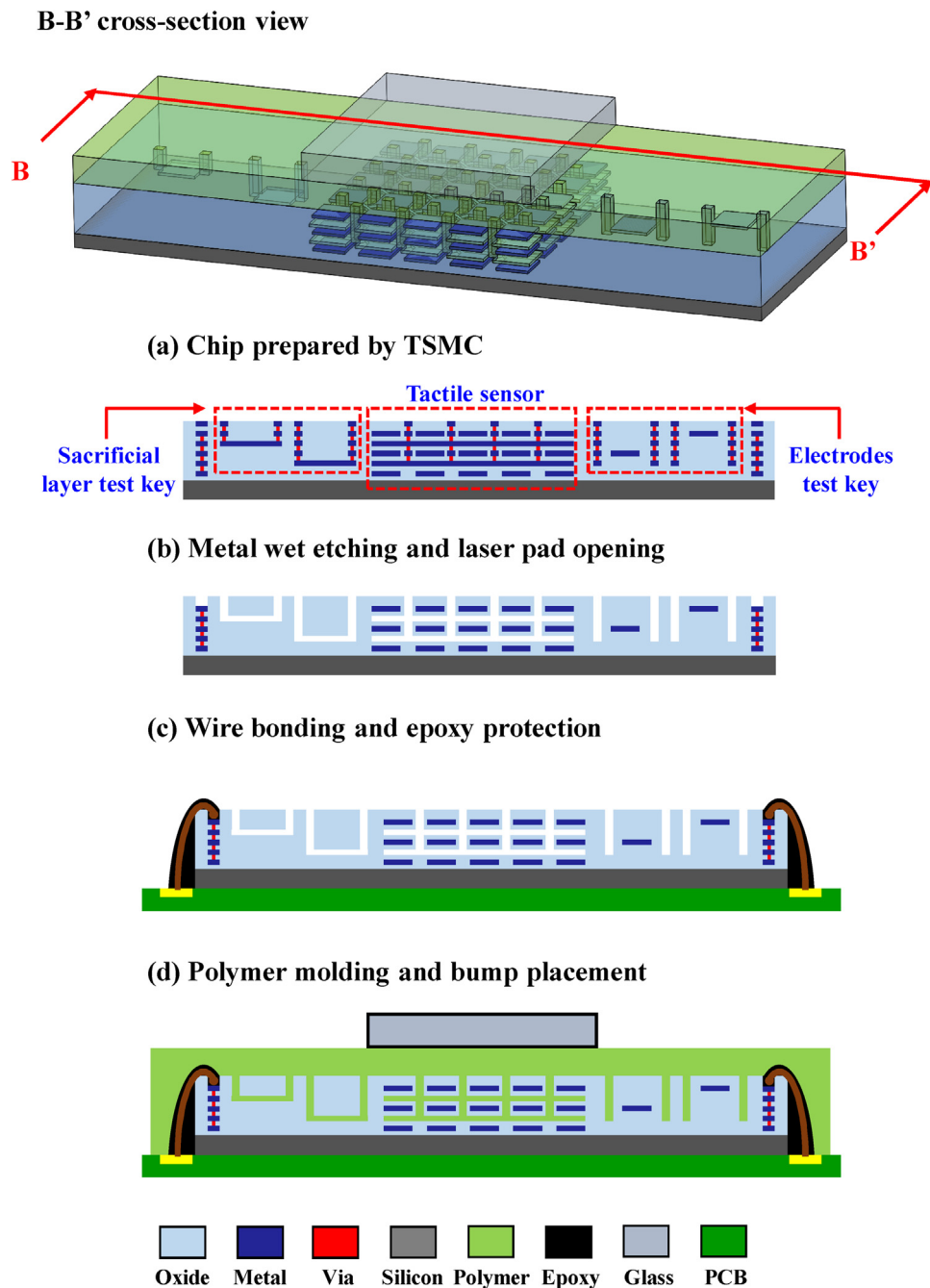


Fig. 5. Schematic illustrations of the proposed fabrication process from the B-B' cross-section view.

Fig. 6 shows the optical microscope (OM), scanning electron microscope (SEM) and focused ion beam (FIB) images of the sensing die before and after metal wet etching (in Fig. 5a and b). The left micrographs in Fig. 6a shows the typical chips prepared by TSMC. Four arrays of tactile sensors and their electrical routings, bonding pads, and etching release holes are observed from each of the two sensing chips. The first chip contains the proposed and reference type tactile sensor to be measured for sensitivity comparison, and the other chip contains the warpage test keys to verify the warpage conditions. Furthermore, the two sensing chips each contain one of the two types of test keys. The alignment marks (metal layer) were designed to assist the following bump assembly process. The right micrograph in Fig. 6a displays the TSMC chips after the metal wet etching and laser trimming (as illustrated in Fig. 5b). It shows the etching release test keys has turned transparent, indicating that the

sacrificial metal layers embedded in between dielectric layers are fully removed. Also, the sensing electrode test keys remained dark, meaning the sensing electrodes have not been attacked. Moreover, the layers inside the etching release holes are removed after the metal wet etching. The nine pads, as indicated by its blackened color, are exposed by laser-machining for wire bonding. The SEM micrographs in Fig. 6b display etching release holes in between sensing units, and the zoom-in micrograph indicates that the layers inside the hole are removed. Micrographs in Fig. 6c exhibit cross sections of the proposed and reference sensing units prepared by the FIB. The ion beam cut at the center of a sensing unit structure reveals the stacked electrodes and their sensing gaps. For the proposed design shown in the left micrograph, the M1, M3 and M5 layers acting as three capacitive sensing electrodes are observed, and the sensing gaps defined after removing M2 and M4 layers can

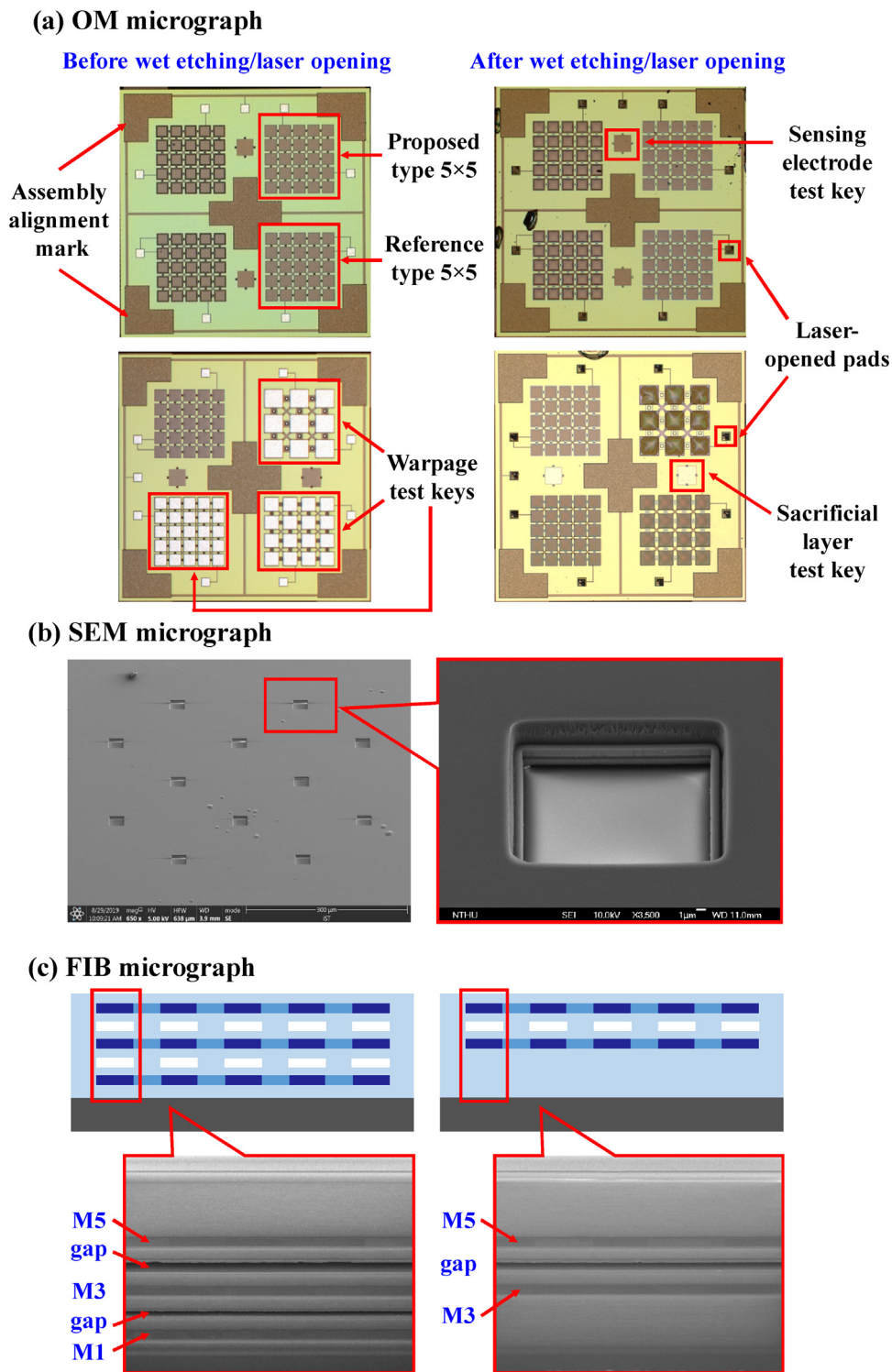


Fig. 6. (a) The OM photos of the overall sensing chips before and after metal etching/laser opening, (b) the SEM micrographs of the tactile sensor array and etching hole zoom in after metal wet etching process, and (c) the FIB micrographs of the released sensing structures with visible sensing gap, metal electrodes, and dielectric layers.

also be seen. The reference design shown in the right micrograph depicts the M3 and M5 electrode layers and their sensing gap. Moreover, the dielectric (silicon dioxide) layers in the lighter shade of gray are also presented in both designs which served to protect the sensing electrodes during the metal wet etching process. Micrographs in Fig. 7 show the sensing die after wire bonding, polymer molding, and bump assembly (in Fig. 5c and d). Fig. 7a depicts the chip on PCB after wire bonding and epoxy protection processes

(in Fig. 5c). Finally, micrographs in Fig. 7b display the polymer-encapsulated chip and wires, and a glass bump is also assembled on the tactile sensing array for testing (associated with the process in Fig. 5d). The rubber O-ring is placed around the sensor to prevent leakage of polymer during molding. The zoom-in micrograph in Fig. 7c shows the 500 μm thick glass bump with planar size of $1000 \times 1000 \mu\text{m}^2$.

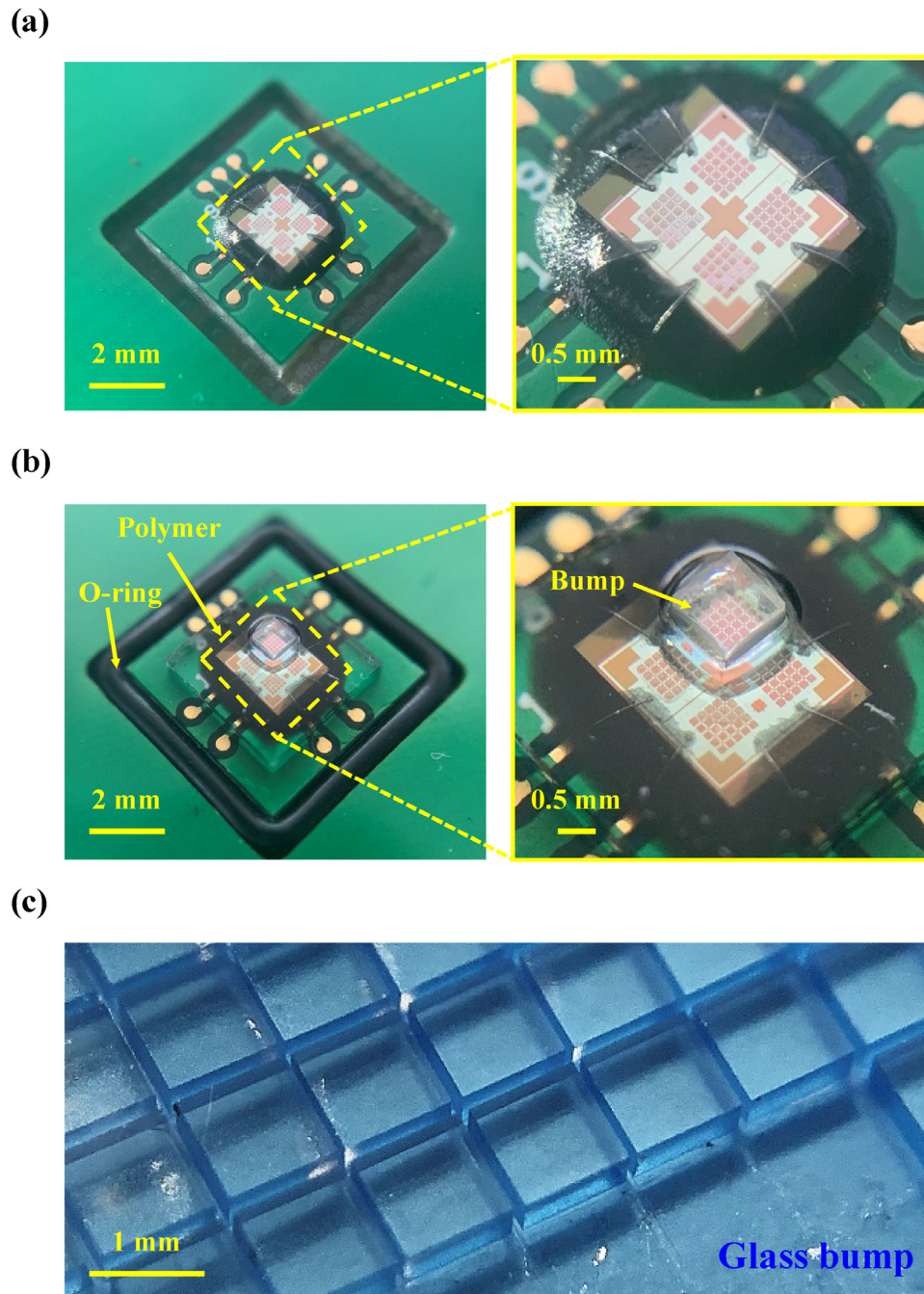


Fig. 7. (a) Overview and zoom-in of the sensor after wire bonding and wire epoxy protection, (b) overview and zoom-in of the sensor after polymer molding with glass bump attached, (c) zoom-in of glass bumps used as contact interface during force loadings.

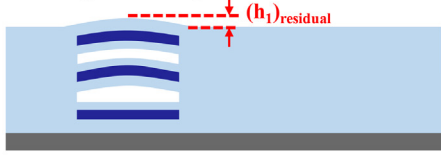
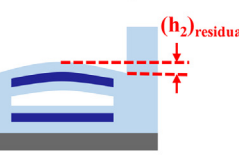
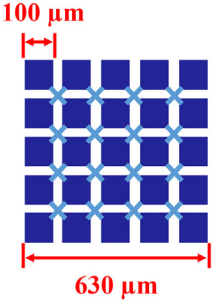
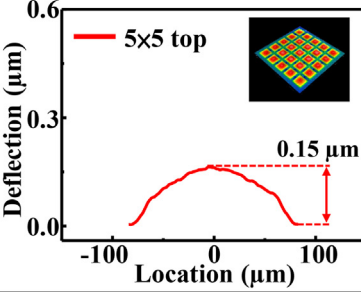
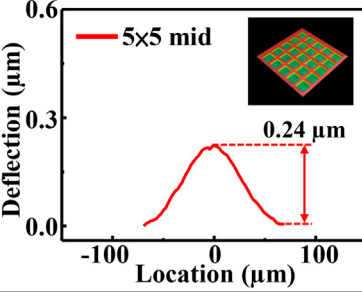
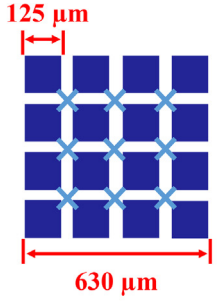
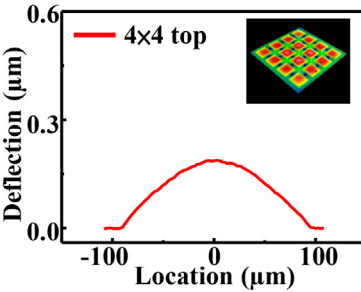
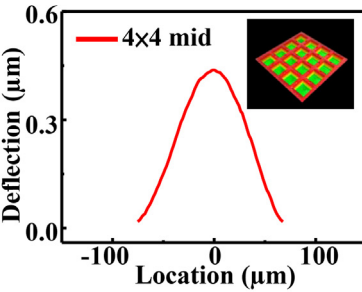
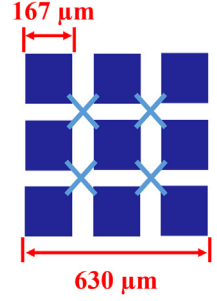
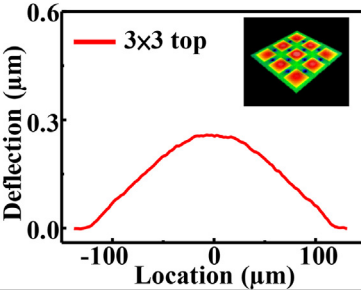
4. Measurement and results

To evaluate the performance of the sensor, several experiments have been conducted. Firstly, to verify the arrayed sensing unit design, proposed types in 3×3 – 5×5 array configurations are compared. Moreover, force responses of both proposed and reference tactile sensor arrays (5×5) are performed for comparison. Note that the reference and proposed designs have identical footprints, sensing unit sizes, gap distances and polymer fill-ins, to establish a fair comparison of sensitivities and sensing ranges. Lastly, due to the employment of polymer, thermal influences on performances of the reference and proposed types have been evaluated.

4.1. Discretized array evaluation

The warpage characterization was carried out with a 3D optical surface profiler (Zygo® Nexview™ NX2) on the released structures (top and middle) of the proposed type tactile sensor in 4×4 and 5×5 array configurations and for the top structure of the 3×3 array. As illustrated in Table 1, test keys were fabricated for the characterization of the top and middle suspended structures. The sensor footprints for both configurations have been fixed at $630 \times 630 \mu\text{m}^2$ (as shown in Fig. 6a), and possesses individual sensing units with in-plane dimensions of $167 \times 167 \mu\text{m}^2$ (for 3×3 array), $125 \times 125 \mu\text{m}^2$ (for 4×4 array) and $100 \times 100 \mu\text{m}^2$ (for 5×5 array). Thus the total sensing area for each array configurations

Table 1
Summarized warpage profile measurements of the top and middle structures for the proposed type tactile sensor in differing array configurations.

Sensors with different arrays	Top test key 	Mid test key 
	 $(h_1)_{residual} : 0.15 \mu\text{m}$	 $(h_2)_{residual} : 0.24 \mu\text{m}$
	 $(h_1)_{residual} : 0.17 \mu\text{m}$	 $(h_2)_{residual} : 0.41 \mu\text{m}$
	 $(h_1)_{residual} : 0.23 \mu\text{m}$	<p style="text-align: center;">N/A (Fabrication failed)</p>

have also been fixed. The measured warpage profiles for the top and middle released structures are presented in Table 1. Results show that by reducing the sensing unit size within the array, the warpage of the membranes can be effectively inhibited for both the middle and the top structure. Note that the thicknesses of middle and top structures are respectively 2.23 μm and 5.63 μm . Thus, for the 4×4 array, the 0.41 μm warpage of the middle structure nearly exceeds the initial gap distance of 0.53 μm , which may create contact issues right after the releasing process. The middle structure warpage for the 3×3 array was unable to be measured due to consistent failures during the releasing process. In summary, the proposed discretized array design could reduce the degree of warpage to improve the process yield and maintain the required gap size for sensing electrodes.

4.2. Vertically stacked design evaluation

The measurement setup in Fig. 8 was established to characterize the force response of the proposed type and reference type tactile sensor. The device-under-test (DUT) was placed on top of a z-axis micro control stage and connected to a commercially available capacitance readout circuit (AD7745/46). A micro force gauge with a resolution of 10 mN and capacity of 50 N is attached to the loading probe and placed directly above the DUT. As can be seen from the zoom-in micrograph in Fig. 8, the loading probe on the force gauge is larger than the glass bump of the DUT, ensuring a uniform distributed load applied on the tactile sensor array. During measurement, the tactile load is specified by the displacement of z-axis stage through the controller, meanwhile the capacitance sig-

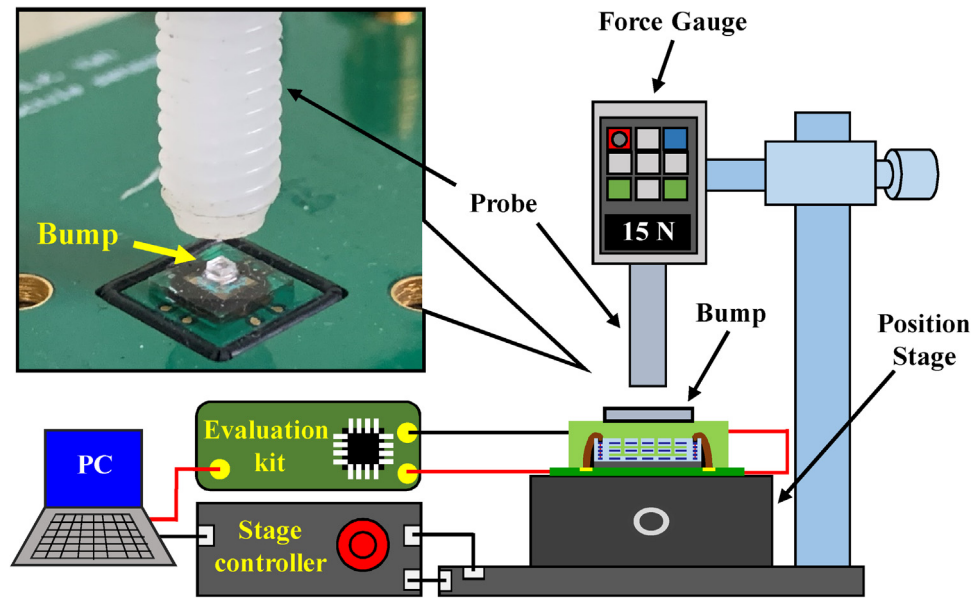


Fig. 8. Measurement setup for characterizing force response of tactile sensors with zoom-in of force loading probe and DUT.

nal from readout circuit and the load from force gauge are recorded. Measurements in Fig. 9a depict typical force responses of the proposed (in red) and reference (in black) designs with 5×5 tactile sensing array. Each measurement point was taken 0.5 N apart, and the error bar represents the results from four measurements to ensure repeatability. According to [18], the measurement range was set at 15 N. Within the 15 N measurement range of the tactile loads, the sensitivities of the proposed and reference designs are respectively 5.62 fF/N and 4.37 fF/N, with initial capacitances of 7.29 pF and 3.39 pF. Thus, the proposed design exhibits a near 1.3-fold enhancement in sensitivity. Moreover, the nonlinearities for both proposed and reference designs are less than 1%. It should be noted there exists discrepancies between the measured and simulated results. The material models and constants used in the simulation has a large impact on the results, and is the main reason for this discrepancy. Using a different set of material constants (Mooney-Rivlin model with $C_{10} = 0.031$ MPa, $C_{01} = 0$ MPa, $C_{11} = 0.027$ MPa and bulk modulus = 962 MPa) measured in a different research [23], will result in significantly different simulation results, as shown in Fig. 9b, where the new set of material constant will lead to underestimation of the sensitivity performance compared to the measurement results. The material constants used for simulation results in Fig. 9b were determined from polymer with thicknesses larger than 100 μm though the curve fitting of experiments [21,23]. These curve fitted constants may not be suited to accurately represent the behavior of the sub-micrometer thick polymer fill-in employed in this research. Therefore, the hyperelastic model parameters may need further modifications for polymers of different geometries in order to achieve more accurate simulation results. Nevertheless, an enhancement in sensitivity can be observed in simulation with both sets of curve-fitted hyperelastic parameters, and further verified by measurement.

4.3. Thermal influence

The effects of thermal influence were also characterized in this study. As shown in Fig. 10a, the heater is added to the measurement setup to provide a change in operating temperature. The measured drift in initial capacitance over the span of 25°C to 85°C is -3.79

fF/°C for the proposed design, and -2.43 fF/°C for the reference design. This equates to temperature coefficient of offsets (TCOs) of -0.05 %/°C for the proposed type and -0.07 %/°C for the reference type, as shown in Fig. 10b. The considerable drifts in initial capacitance is due to the high coefficient of thermal expansion (CTE, 340 ppm/°C) of the employed polymer within the gaps of the capacitors. The expanding polymer fill-in within the capacitor gaps during thermal influences will enlarge the gap heights between sensing electrodes which in turn lowers the initial capacitance. Measurements in Fig. 11 further show the thermal influences on the force responses for both the proposed and reference designs. The results indicate that the sensitivity will increase with the heater temperature. As the heater temperature increased from 25°C to 85°C, the sensitivity of proposed design (in Fig. 11a) increased from 5.62 fF/N to 7.74 fF/N, and the sensitivity of reference design (in Fig. 12b) increased from 4.37 fF/N to 6.37 fF/N. As summarized in Fig. 11c, the measured sensitivities show a 37% and 45% increase for the proposed type and reference type across a 60°C span, so that the temperature coefficient of sensitivity (TCS) of the proposed and reference designs are 0.63 %/°C and 0.75 %/°C respectively. The significant TCSs for both types of tactile sensors should be noted for employment in applications of varying operating or target temperature, as it may have a considerable effect on the force readings in such environments.

5. Conclusions

This study presents a tactile sensor featuring vertically stacked structures which was demonstrated to show an enhancement in sensitivity without sacrificing footprint area. Also, the sensor was discretized into an array to mitigate warpage problems arising from thin film residual stress. By employing a parallel configuration for the sensing units in the array, the capacitance change signal of every sensing unit, ΔC_{unit} , can contribute to the overall signal output. The designs of this study was possible due to the multi-layers stacking and great electrical routing capability of the CMOS platform. Sensing electrodes can be vertically integrated and electrically connected while maintaining the same device footprint. In this study, PDMS polymer was employed as a polymer buffer above

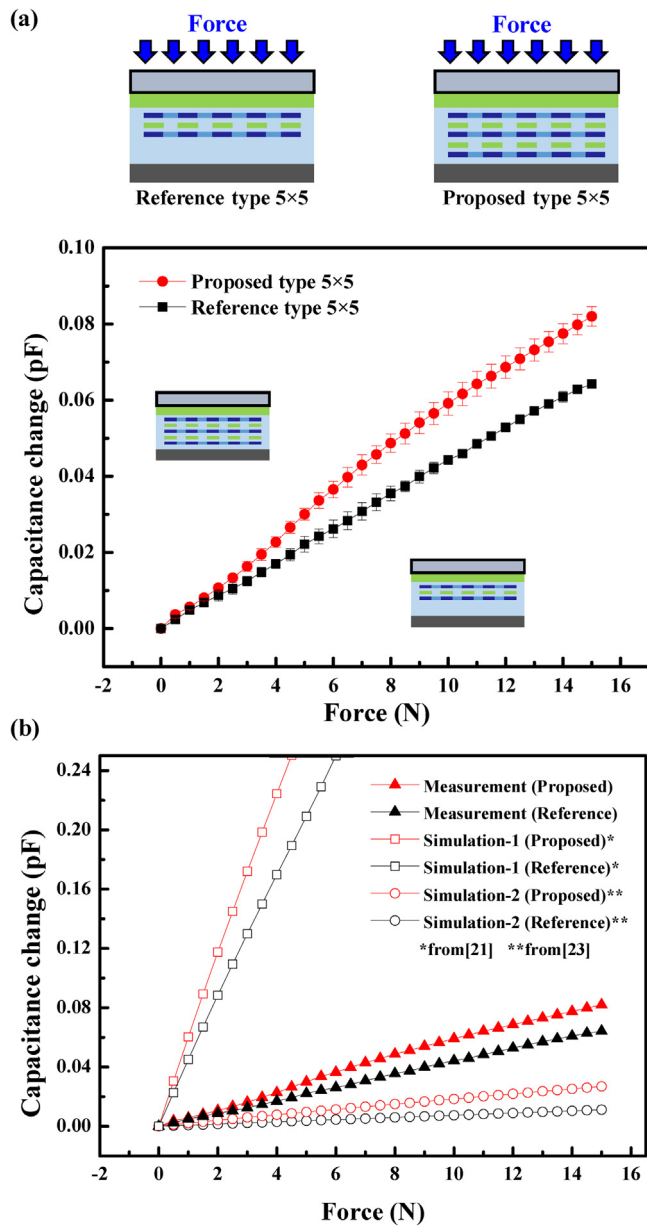


Fig. 9. (a) Measurement results for the force response of proposed and reference type tactile sensors, and (b) the comparisons of simulation results with different hyperelastic material constants with the measured results. *Simulation-1 results with material constants from [21]. **Simulation-2 results with material constants from [23].

the sensor and as polymer fill-ins between the gaps of the vertically integrated structures for force transmission. Employment of the polymer buffer effectively loads force onto the sensor, and the polymer fill-in enables simultaneous deformation of the released structures. The simultaneous deformation results in a larger capacitance change output due to the summing of signals from vertically integrated sensing pairs. Proposed type sensor array configurations with different sensing unit sizes were investigated in the measurement results. Warpage measurements for different configurations showed an effective inhibition of residual stress warpage by reducing the size of the discretized sensing unit. The array configurations

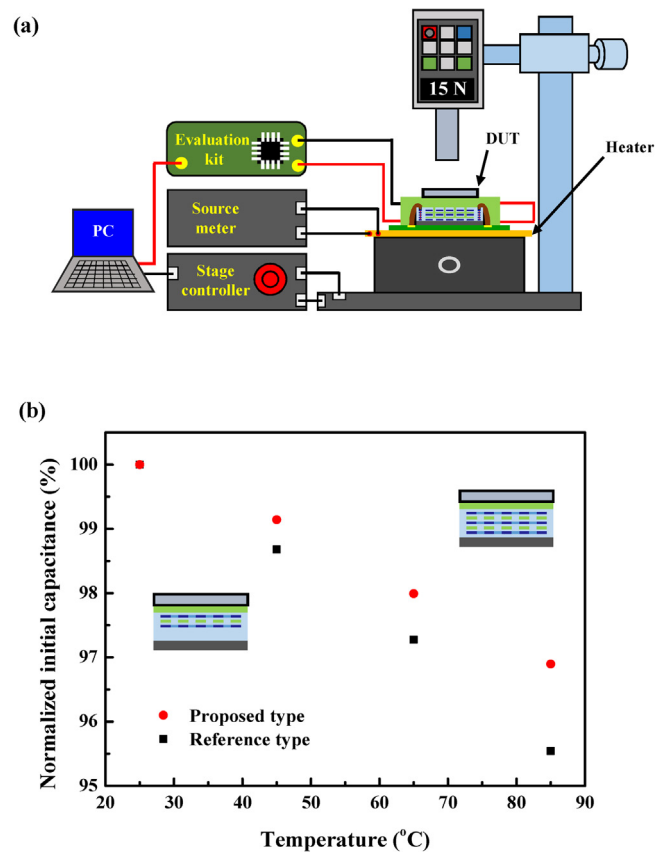


Fig. 10. (a) The measurement setup for thermal influences on the tactile sensor, and (b) measurement results of temperature effect on reference and proposed type tactile sensor initial capacitances C_0 .

with larger unit sizes showed more severe residual stress warpings and even possible fabrication failures. Next, within the loading range specification of 0~15 N, measurement results showed an enhanced sensitivity of 5.61 fF/N for the proposed type sensor, compared to a sensitivity of 4.37 fF/N for reference type. Lastly, characterizations of the thermal influences for the two types of tactile sensors were performed. Measurements indicated the proposed type sensor has a better TCO of $-0.05\%/^{\circ}\text{C}$ as compared with the reference type sensor of $-0.07\%/^{\circ}\text{C}$, which was contributed by the three vertically integrated structures design. Moreover, force response measurements under different temperatures within 25–85°C revealed TCSs of 0.63 $\%/^{\circ}\text{C}$ and 0.75 $\%/^{\circ}\text{C}$ respectively for the proposed type and reference type tactile sensor. Due to the employment of polymer in this study, significant TCOs and TCSs were measured for both types of sensors. In fact, the same problem may happen to other tactile sensors consisted of polymer layers or fill-in. As such, for future real applications, the thermal influences on the employed polymers and its effect on performance should be carefully taken into account.

CRedit authorship contribution statement

Meng-Lin Hsieh: Conceptualization, Methodology, Investigation, Writing - original draft. **Sheng-Kai Yeh:** Visualization, Methodology, Investigation, Writing - review & editing. **Jia-Horng Lee:** Conceptualization, Investigation. **Ming-Ching Cheng:** Conceptualization, Software. **Weileun Fang:** Supervision, Resources, Writing - review & editing, Project administration.

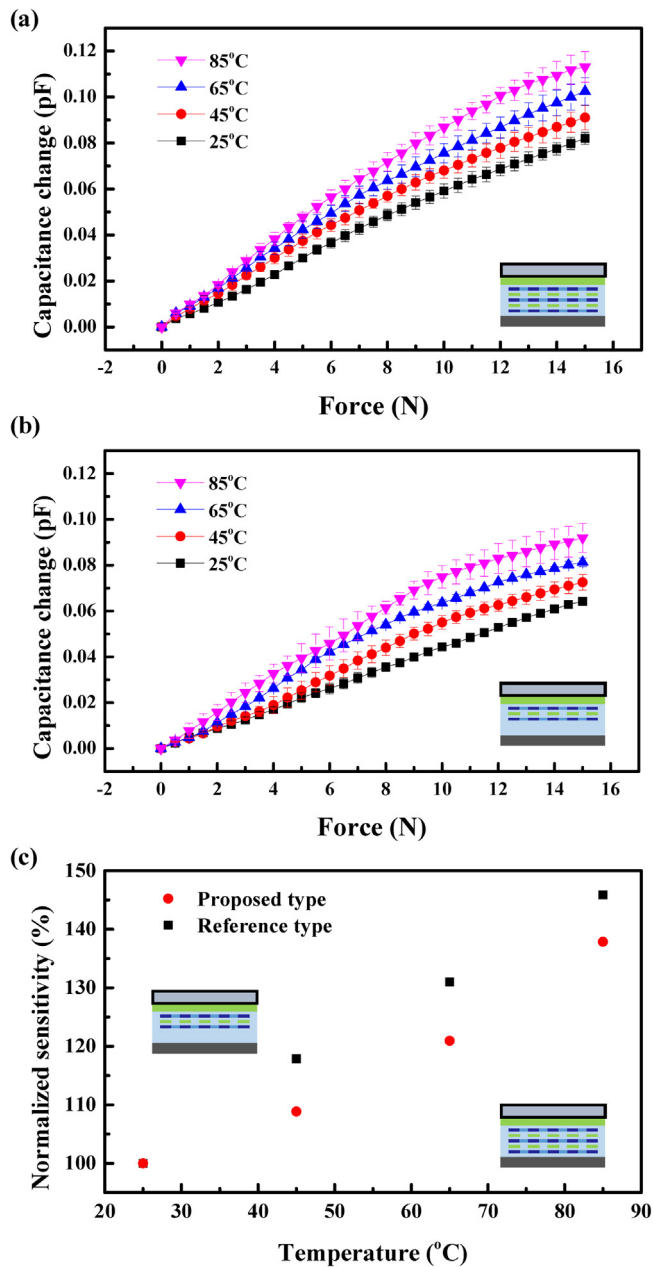


Fig. 11. Thermal influence on the force response (ΔC) for (a) the proposed type tactile sensor, (b) the reference type tactile sensor, and (c) the normalized sensitivities for both the proposed and reference types under different operating temperatures.

Declaration of Competing Interest

None.

Acknowledgements

This project was supported by the Ministry of Science and Technology (MOST) of Taiwan under the grant number MOST 108-2218-E-007-034-. The authors would also like to appreciate the Taiwan Semiconductor Manufacturing Company (TSMC) and the Taiwan Semiconductor Research Institute (TSRI), for the supporting of CMOS chip manufacturing. The authors also appreciate the Center for Nanotechnology, Materials Science and Microsystems (CNMM) of National Tsing Hua University for providing the tools in the processes. Lastly, warmest thanks to the lab members of Micro Device Laboratory from NTHU for their invaluable assistance.

References

- [1] Apple Inc, "Earbuds with capacitive touch sensor", United States Patent 10 003 881, June 19, 2018.
- [2] S.-K. Yeh, H.-C. Chang, W. Fang, Development of CMOS MEMS inductive type tactile sensor with the integration of chrome steel ball force interface, *J. Micromech. Microeng.* 28 (4) (2018) 044005.
- [3] T.-V. Nguyen, R. Tani, T. Takahata, I. Shimoyama, Development of a single-chip elasticity sensor using MEMS-based piezoresistive cantilevers with different tactile properties, *Sens. Actuators A Phys.* 285 (2019) 362–368.
- [4] H. Takao, M. Yawata, K. Sawada, M. Ishida, A multifunctional integrated silicon tactile imager with arrays of strain and temperature sensors on single crystal silicon diaphragm, *Sens. Actuators A Phys.* 160 (1–2) (2010) 69–77.
- [5] R.S. Dahiya, M. Valle, *Robotic Tactile Sensing*, Springer, New York, 2013, pp. 9.
- [6] W.-C. Lai, W. Fang, Novel two-stage CMOS-MEMS capacitive-type tactile-sensor with ER-fluid fill-in for sensitivity and sensing range enhancement, *Transducers* (2017) 1175–1178.
- [7] S.-Y. Tu, W.-C. Lai, W. Fang, Vertical integration of capacitive and piezo-resistive sensing units to enlarge the sensing range of CMOS-MEMS tactile sensor, *IEEE MEMS* (2017) 1048–1051.
- [8] Y.-C. Liu, C.-M. Sun, L.-Y. Lin, M.-H. Tsai, W. Fang, Development of a CMOS-based capacitive tactile sensor with adjustable sensing range and sensitivity using polymer fill-in, *J. Microelectromech. Syst.* 20 (1) (2011) 119–127.
- [9] Y.-H. Gao, Y.-H. Jen, R. Chen, K. Aw, D. Yamane, C.-Y. Lo, Five-fold sensitivity enhancement in a capacitive tactile sensor by reducing material and structural rigidity, *Sens. Actuators A Phys.* 293 (2019) 167–177.
- [10] J. Kim, T.N. Ng, W.S. Kim, Highly sensitive tactile sensors integrated with organic transistors, *Appl. Phys. Lett.* 101 (10) (2012) 103308.
- [11] S.C.B. Mannsfeld, B.C. Tee, R.M. Stoltenberg, C.V.H. Chen, S. Barman, B.V.O. Muir, A.N. Sokolov, C. Reese, Z. Bao, Highly sensitive flexible pressure sensors with microstructured rubber dielectric layers, *Nat. Mater.* 9 (10) (2010) 859–864.
- [12] N.A. Ridzuan, S. Masuda, N. Miki, Flexible capacitive sensor encapsulating liquids as dielectric with a largely deformable polymer membrane, *Micro Nano Lett.* 7 (12) (2012) 1193–1196.
- [13] Y. Huang, H. Yuan, W. Kan, X. Guo, C. Liu, P. Liu, A flexible three-axial capacitive tactile sensor with multilayered dielectric for artificial skin applications, *Microsyst. Technol.* 23 (6) (2017) 1847–1852.
- [14] C.-M. Sun, C. Wang, W. Fang, On the sensitivity improvement of CMOS capacitive accelerometer, *Sens. Actuators A Phys.* 141 (2) (2008) 347–352.
- [15] H. Xie, G.K. Fedder, Vertical comb-finger capacitive actuation and sensing for CMOS-MEMS, *Sens. Actuators A Phys.* 95 (2–3) (2002) 212–221.
- [16] J.-H. Lee, S.-K. Yeh, W. Fang, Monolithic/vertical integration of piezo-resistive tactile sensor and inductive proximity sensor using CMOS-MEMS technology, *IEEE MEMS* (2019) 826–829.
- [17] M.-L. Hsieh, S.-K. Yeh, J.-H. Lee, P.-S. Lin, M.-F. Lai, W. Fang, Vertically integrated multiple electrode design for sensitivity enhancement of CMOS-MEMS capacitive tactile sensor, *Transducers* (2019) 2174–2177.
- [18] R.S. Dahiya, G. Metta, M. Valle, G. Sandini, Tactile sensing—from humans to humanoids, *IEEE Trans. Robot.* 26 (1) (2009) 1–20.
- [19] W. Fang, J. Wickert, Determining mean and gradient residual stresses in thin films using micromachined cantilevers, *J. Micromech. Microeng.* 6 (3) (1996) 301.
- [20] C.-L. Cheng, M.-H. Tsai, W. Fang, Determining the thermal expansion coefficient of thin films for a CMOS MEMS process using test cantilevers, *J. Micromech. Microeng.* 25 (2) (2015) 025014.
- [21] S.-K. Yeh, J.-H. Lee, W. Fang, On the detection interfaces for inductive type tactile sensors, *Sens. Actuators A Phys.* 297 (2019) 111545.
- [22] M.-H. Tsai, C.-M. Sun, Y.-C. Liu, C. Wang, W. Fang, Design and application of a metal wet-etching post-process for the improvement of CMOS-MEMS capacitive sensors, *J. Micromech. Microeng.* 19 (10) (2009) 105017.
- [23] T.K. Kim, J.K. Kim, O.C. Jeong, Measurement of nonlinear mechanical properties of PDMS elastomer, *Microelectron. Eng.* 88 (8) (2011) 1982–1985.

Biographies



Meng-Lin Hsieh was born in Taipei, Taiwan. He received his B.S. and M.S. degree from the Department of Power Mechanical Engineering, National Tsing Hua University, Taiwan. He is currently a research assistant in the Department of Power Mechanical Engineering, National Tsing Hua University, Taiwan. His research interest includes the design of CMOS-MEMS tactile sensors and the application of polymer for micro tactile sensors.



Sheng-Kai Yeh was born in Taichung, Taiwan. In 2016, he received his B.S. degree from the Department of Power Mechanical Engineering, National Tsing Hua University, Taiwan. In 2017, he received his M.S. degree from the Department of Power Mechanical Engineering, National Tsing Hua University, Taiwan. He is currently a Ph.D. student in the Department of Power Mechanical Engineering, National Tsing Hua University, Taiwan. His research interests include design and implementation of the micro tactile sensor, contact interface design/integration of the micro tactile sensor, and the implementation of CMOS-MEMS sensors.



Jia-Horng Lee was born in Kaohsiung, Taiwan. In 2017, he received his B.S. degree from the Department of Power Mechanical Engineering, National Tsing Hua University, Taiwan. In 2019, he received his M.S. degree from the Department of Power Mechanical Engineering, National Tsing Hua University, Taiwan. His research interests include design of the tactile sensor and integration of tactile sensor and proximity sensor.



Ming-Ching Cheng was born in Taipei, Taiwan. In 2018, he received his B.S. degree from the Interdisciplinary Program of Nuclear Science, National Tsing Hua University, Taiwan. He is currently an M.S. student in the Department of Power Mechanical Engineering, National Tsing Hua University, Taiwan. He is currently researching on Fabry-Perot interferometer(FPI) and is familiar with fabrication process of Si-based wafer, including surface- and bulk-micromachining.



Weileun Fang was born in Taipei, Taiwan. He received his Ph.D. degree from Carnegie in 1995. His doctoral research focused on the determining of the mechanical properties of thin films using micromachined structures. In 1995, he worked as a postdoctoral research at Synchrotron Radiation Research Center. He joined the Power Mechanical Engineering Department at the National Tsing Hua University (Taiwan) in 1996, where he is now a Chair Professor as well as a faculty of NEMS Institute. In 1999, he was with Prof. Y.-C. Tai at California Inst. Tech. as a visiting associate. He became the IEEE Fellow in 2015 to recognize his contribution in MEMS area. His research interests include MEMS with emphasis on micro fabrication/packaging technologies, CMOS MEMS, CNT MEMS, micro optical systems, micro sensors and actuators, and characterization of thin film mechanical properties. He is now the Chief Editor of JMM, the Associate Editor of IEEE Sensors Journal, and the Board Member of IEEE Transactions on Device and Materials Reliability. He served as the member of ISC (International steering committee) of Transducers in 2009–2017, and the ISC chair in 2017–2019. He also served as the General Chair of Transducers Conference in 2017. He was the TPC of IEEE MEMS and EPC of Transducers for many years, and the Program Chair of IEEE Sensors Conference in 2012. He served as the Chief Delegate of Taiwan for the World Micromachine Summit (MMS) in 2008–2012, and the General Chair of MMS in 2012. Prof. Fang has close collaboration with MEMS industries and is now the VP of MEMS and Sensors Committee of SEMI Taiwan.